678. Vibration analysis and control in linear switched reluctance motor

N. C. Lenin[1], R. Arumugam[2]
[1] Department of Electrical Engineering, St. Joseph's College of Engineering, Chennai, Tamilnadu, India
[2] Department of Electrical Engineering, SSN College of Engineering, Chennai, Tamilnadu, India
E-mail: *nclenin@gmail.com*

(Received 28 August 2011; accepted 4 December 2011)

Abstract. Vibration is one of the major drawbacks of Linear Switched Reluctance Motor (LSRM). Two design techniques to reduce vibration in the LSRM are proposed. A detailed mathematical approach for calculating natural frequency has been outlined. Different techniques to predict the vibration frequencies are analyzed using ANSYS software. The analyzed structures are compared by using experimental and simulation results.

Keywords: linear motor, vibration, modal analysis, FFT, structural harmonic analysis.

1. Introduction

Vibrations, and consequently the noise generated by an electrical machine, can be reduced if the forces produced during their operation are not allowed to excite any resonances of the machine [1]. An accurate determination of the vibration characteristics and the resonant frequencies of stators of electrical machines is, therefore, very important. Often it is impossible to avoid excitation of resonances at all operating conditions, such as under variable frequency operation of electrical motors [2]. By using a vibration model, a designer can predetermine the resulting vibrations and hence optimize the motor design from the perspective of noise and vibrations [3]. From the vibration point of view, the stator of an electrical machine can be modeled as a system consisting of a number of masses interconnected by springs and damping elements to facilitate the analytical solution of the dynamic behavior of the structure. The distribution of the mass and stiffness, which are essential to the determination of the resonances, are well documented in the literature [4-6].

1. Linear Switched Reluctance Motor

2.1. Introduction

A LSRM is an electrical machine in which the force is developed by the tendency of the translator to occupy a position so as to minimize the reluctance of the magnetic path of the excited stator phase winding. A two dimensional (2-D) model of a basic LSRM is shown in Fig. 1. The specifications and dimensions of the basic machine are listed in Table 1. In this paper 2-D FEA has been carried out on the machine depicted in Fig. 1, using FEA based CAD package MagNet.

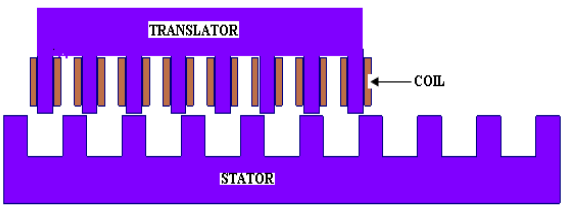

Fig. 1. 2D cross-sectional view of the basic LSRM

Table 1. Specifications and dimensions of the studied LSRM

Air gap length = 3 mm	Width of the stator pole = 16 mm
Maximum force (F_{max}) = 36 N	Height of the stator pole = 19 mm
Stack length = 40 mm	Width of the stator slot = 24 mm
Steel type (Stator) - M 45	Width of the translator slot = 18 mm
Steel type (Translator) - M 45	Height of the translator pole = 75 mm
Travel length= 2 m	Width of the translator pole = 12 mm
Rated voltage = 120 V	Converter switching frequency = 1200 Hz
Rated current = 8 A	Converter type = Classical bridge converter

2. 2. Electromagnetic results

The field analysis has been carried out for a phase excitation of 8 Amps. LSRM is moved from the unaligned position to aligned position. The predicted propulsion and normal force profiles are presented in Figs. 2 and 3 respectively.

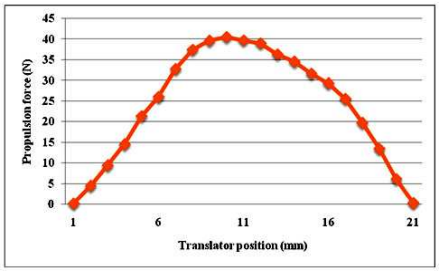

Fig. 2. Propulsion force vs. translator position

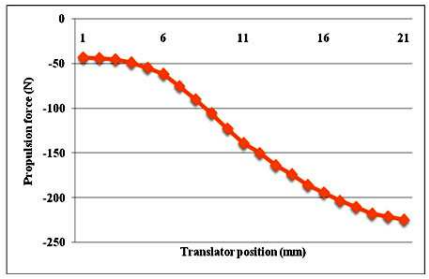

Fig. 3. Normal force vs. translator position

3. Proposed stator structures

Two stator structures are proposed to mitigate the vibration of the LSRM. In the proposed structures the stator has (a) inter poles and (b) pole shoes illustrated in Figs. 4 and 5 respectively.

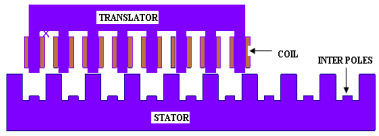

Fig. 4. 2-D cross-sectional view of the proposed LSRM with inter poles

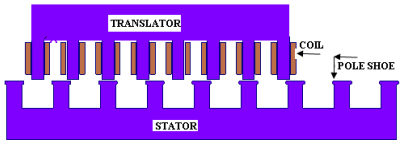

Fig. 5. 2-D cross-sectional view of the proposed LSRM with pole shoes

3. 1. Stator with inter poles

Fig. 4 shows the LSRM stator with inter poles. The width and height of the inter pole is 8 mm and 10 mm respectively. The field analysis has been carried out for an excitation of 8

Amps. The predicted propulsion, and normal force profiles are shown in Figs. 6 and 7 respectively.

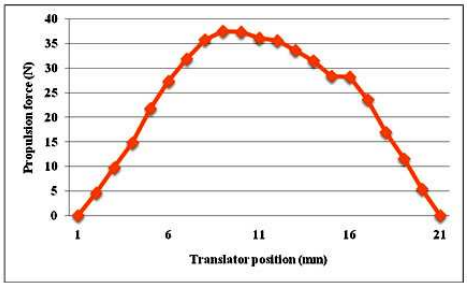

Fig. 6. Propulsion force vs. translator position

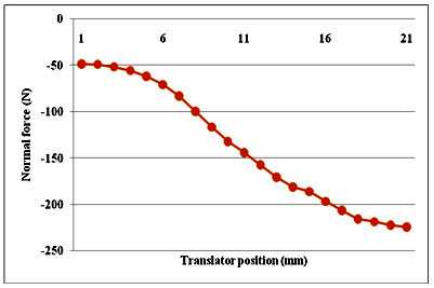

Fig. 7. Normal force vs. translator position

3. 2. Stator with pole shoes

The aim in proposing the stator pole shoe is to widen the stator pole width and to smoothen the force profile. The analysis is carried out on the basic LSRM with a pole shoe, which is affixed on the stator poles. The width of the stator pole shoe is fixed to 4 mm. The mutual inductance and leakage effects are neglected. The simulation is presented for an excitation current of 8 Amps. The predicted propulsion force, and normal force profiles are shown in Figs. 8 and 9 respectively. Table 4 shows the comparison of the basic and proposed structures.

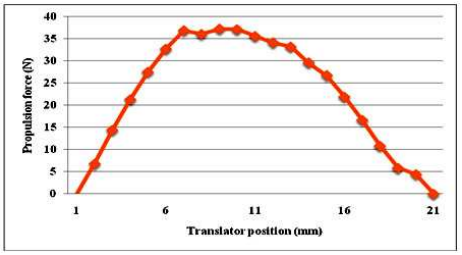

Fig. 8. Propulsion force vs. translator position

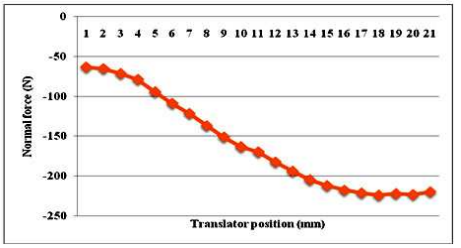

Fig. 9. Normal force vs. translator position

Table 2. Comparison of basic and proposed structures

	Basic structure	Stator with inter poles	Stator with pole shoes
Peak propulsion force (N)	38.958	37.539	38.623
Average propulsion force (N)	35.961	34.720	35.383
Peak normal force (N)	-224.074	-223.851	-223.351

4. Vibration analysis

4. 1. Introduction

The low frequency range of the vibrational energy, which is not audible at all (f<30Hz), or is audible but with considerable damping by the ear (f<1000 Hz), is called the vibration of the machines. The vibrating capacity of the machine is a function of two parameters, namely the vibration mode number and frequency. At least one natural frequency of the machine corresponds to each vibration mode. A dangerous situation arises where the frequency of the periodic exciting force is identical to or close to one of the natural frequencies of the machine.

The causes of vibrations in the LSRM are:

- Force ripples.
- Magnetic forces acting on the stator surfaces.
- Current harmonics.

In this section, three stator structures are investigated to study their vibration behavior. Initially, the vibration frequencies and their magnitudes due to the force ripple are estimated from the electromagnetic force, using the Fast Fourier transform (FFT). From the geometry of the motor, the natural vibration frequencies of the LSRM are estimated using the 2-D modal analysis. The vibrations of the stator structure due to the current harmonics are calculated using the 3-D structural harmonic analysis. Finally, an experiment is carried out on the studied structures to compare the estimated vibration frequencies with the measured values. The results from the electromagnetic field analysis, performed in section 2 and 3 have been adopted for vibration analysis in this section.

4. 2. Vibration due to force ripple

From the results of the 2-D finite-element field analysis performed earlier, the force versus translator position will be known. A program is written in a MATLAB environment, which contains a sequence of instructions to store the array of the four phases. The dynamic force obtained is shown in Fig. 10.

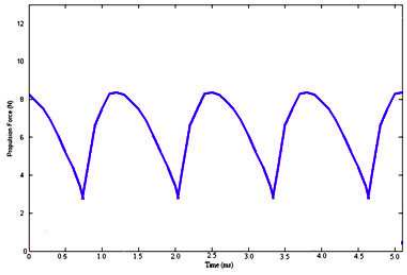

Fig. 10. Dynamic electromagnetic force

The FFT is applied to the net force profile after the elimination of the dc offset. Since the FFT transforms the available data in the time domain into the frequency domain, the available force versus translator position profile must be converted into the force versus time profile. In MATLAB, the command fft (*x*, *p*), where '*x*' is the force array and '*p*' is 512, denoting the 512 point FFT will be solved to produce a complex Discrete Fourier transform (DFT) of force. The absolute value of the obtained complex DFT will form the magnitude axis. The magnitude plot is obtained by plotting the magnitude versus frequency. The block diagram for the FFT analysis is shown in Fig. 11.

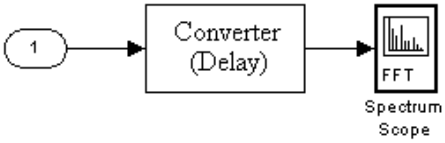

Fig. 11. MATLAB model of FFT function

Fig. 12 shows the results of the frequency spectrum analysis for the case of the basic stator. The frequency corresponding to these decibel (dB) peaks can be identified from the plot. Table 3 lists the dominant frequencies in hertz (Hz) and its amplitude in dB. Similarly, the results of the FFT for the LSRM with pole shoes and with inter poles are depicted in Fig. 13. It is observed from the Table 3. that the dB peaks occurs at certain frequencies but the magnitude of the dB peaks is reduced by considerable margin, in both proposed structures.

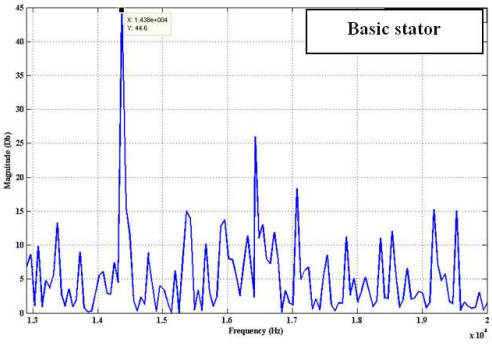

Fig. 12. FFT output: dB vs. frequency, for the basic structure

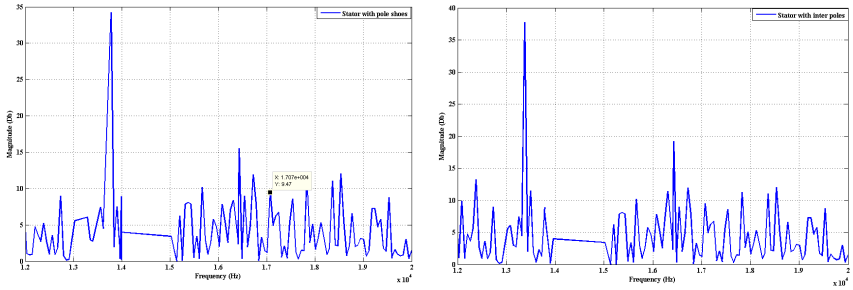

Fig. 13. FFT output: dB vs. frequency, for the LSRM with pole shoe and inter poles

Table 3. Dominant ripple frequencies and its amplitude

a. Basic stator

Predominant ripple frequencies (Hz)	Amplitude (dB)
14385	44.6
16436	25.96
17071	18.37

b. Stator with pole shoe

Predominant ripple frequencies (Hz)	Amplitude (dB)
13783	34.24
16436	15.52
17071	9.47

c. Stator with inter poles

Predominant ripple frequencies (Hz)	Amplitude (dB)
13385	37.74
16436	19.23
16724	11.92

4. 3. Estimation of natural resonance frequencies

We assume that the LSRM behaves as a simple rectangular beam with a distributed load with the base fixed. To determine the natural frequencies, f_n of the rectangular structure, analytically, the following equations are used:

$$f_n = \frac{1}{2\pi}\sqrt{\frac{k_s}{m}}\ \text{Hz} \quad (1)$$

where m - equivalent mass per square meter (Kg/m^2), k_s - spring stiffness coefficient, given by:

$$k_s = \frac{192 \cdot E \cdot I}{l^3} \quad (2)$$

where E - Young's modulus ($E = 2.07 \cdot 10^{11} \text{N/mm}^2$), I - moment of inertia, given by:

$$I = \frac{b \cdot h^3}{12} \text{Kg.m}^2 \quad (3)$$

Mass of the stator without slots (rectangular beam), M_s = 20 Kg, f_n = 9,287.65 Hz, mass of the stator with slots is 12.8 Kg, f_n = 11,609.56 Hz.

4. 4. Calculation of natural frequencies on the stator Using 2-D FEA

Mode shapes and resonant frequencies were computed with the ANSYS finite element analysis platform. The goal of the modeling was the calculation of the set of five eigen-modes. The following steps are used to perform 2-D modal analysis in ANSYS platform:

- Step 1: Set preferences.
- Step 2: Model the stator.
- Step 3: Define material properties.
- Step 4: Define element types.
- Step 5: Mesh the area.
- Step 6: Apply Loads.
- Step 7: Solve.
- Step 8: Review Results and List the natural frequencies.

The material properties used in this analysis are density ρ = 7700 kg/m^3, Young's modulus, E = 207 GPa, Poisson's ratio, ν = 0.3. The computed 2-D mode shapes for the basic and the proposed structures are presented graphically in Figs. 14-16. The comparisons of the stator mode frequencies are provided in Table 4.

Table 4. Comparison of 2-D stator mode frequencies

Mode no.	Frequencies (Hz)		
	Basic structure	Stator with pole shoes	Stator with Inter poles
1	14259	13713	13512
2	14261	13744	13518
3	17466	16918	16468
4	17517	16960	16515
5	17599	17035	16585

From the above analysis the stator mode frequencies of the proposed structures are approximately 4% less, when compared to the basic structure.

4. 5. Vibration due to magnetic forces

In LSRM there are two forces acting on the stator:

- Normal force.
- Tangential force.

The tangential force is the one that acts along the surface as shown in Fig. 17. Normal force is the one that acts perpendicular to the stator or translator surface as shown in Fig. 18. The magnetic forces are calculated using Maxwell's stress tensor method. The normal and tangential forces acting on the stator pole face are depicted in Figs. 19 and 20 respectively.

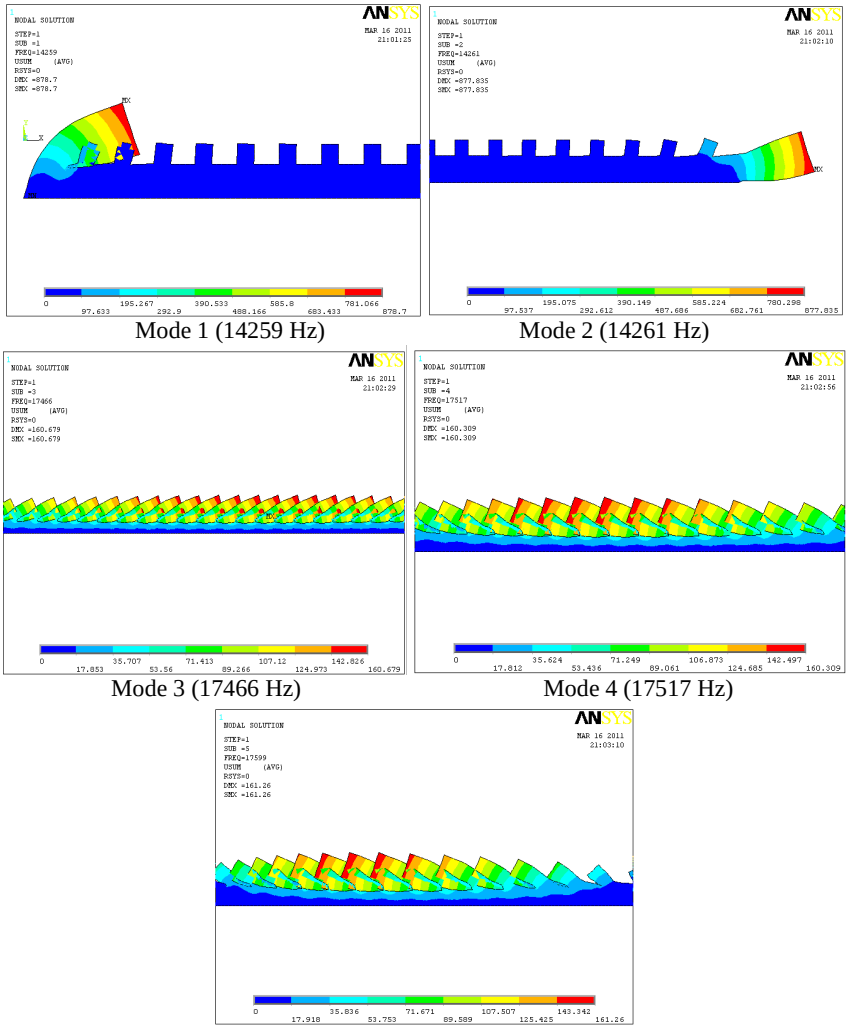

Mode 1 (14259 Hz) Mode 2 (14261 Hz)

Mode 3 (17466 Hz) Mode 4 (17517 Hz)

Mode 5 (17599 Hz)

Fig. 14. 2-D Mode shapes for the basic structure

It is observed from the profiles that, the normal force has a maximum value when the translator is in aligned position. The tangential force is maximum in the overlapping area where as it is minimum in the aligned and unaligned position.

4. 5. 1. Estimation of vibration due to magnetic forces on the stator

The estimated current and normal force on the stator side during dynamic operating condition is shown in Fig. 21. The FFT function block, presented in Fig. 11, is used to find the vibration frequencies and their magnitudes. Fig. 22 shows the spectrum of frequencies due to the normal force on the stator. It is observed that at 12367 Hz and 14256 Hz the magnitude of the normal force is high.

The estimated current and tangential force on the stator side during dynamic operating condition is provided in Fig. 23. The spectrum of the tangential force is given in the Fig. 24. It is

observed that the magnitude of the tangential force is high at the frequencies 4627 Hz, 12621 Hz and 14432 Hz from the spectrum.

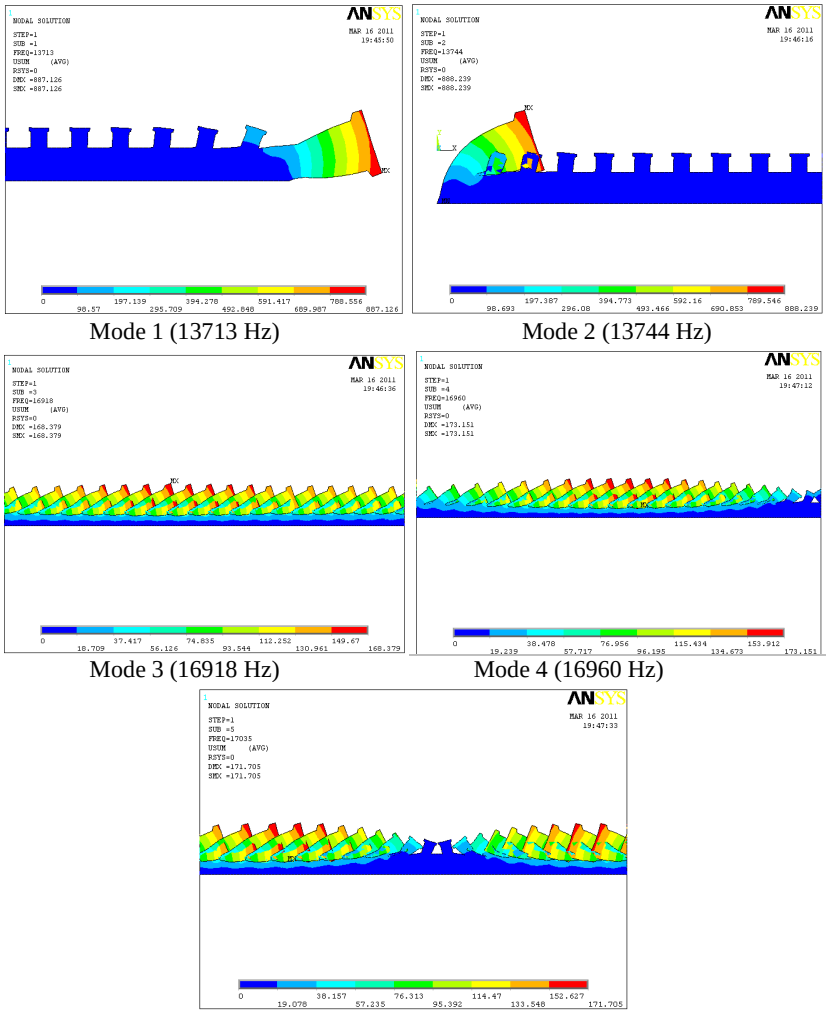

Mode 1 (13713 Hz) Mode 2 (13744 Hz)

Mode 3 (16918 Hz) Mode 4 (16960 Hz)

Mode 5 (17035 Hz)

Fig. 15. 2-D Mode shapes for the stator with pole shoes

4. 6. Estimation of Vibration on the Stator Using Structural Harmonic FEA

4. 6. 1. Introduction

Vibrations are estimated using the 3-D structural harmonic analysis in this section. The magnetic forces calculated using 2-D electromagnetic FEA has been used as input to the structural harmonic FEA to calculate the vibration. The steps involved in the structural harmonic analysis are:

- The normal and tangential forces are calculated using the 2-D electromagnetic FEA.
- To conduct the harmonic structural analysis in 3-D, the 2-D mesh created during the electromagnetic FEA is swapped using ANSYS commands and the element type is changed from PLANE53 to SOLID45.

- The degrees of freedom used for the electromagnetic 2-D FEA (AZ) is changed to structural degrees of freedom (UX, UY, UZ) by changing the element type from PLANE53 to SOLID45.
- The material properties (mass density, Poisson's ratio, Young's modulus) required for the structural analysis are defined for the stator volume.
- The stator is fixed on the base by selecting the nodes on the surface and applying the displacement on these nodes as zero.
- The magnetic forces calculated from the electromagnetic 2-D analysis are applied to the inner surface of the stator.

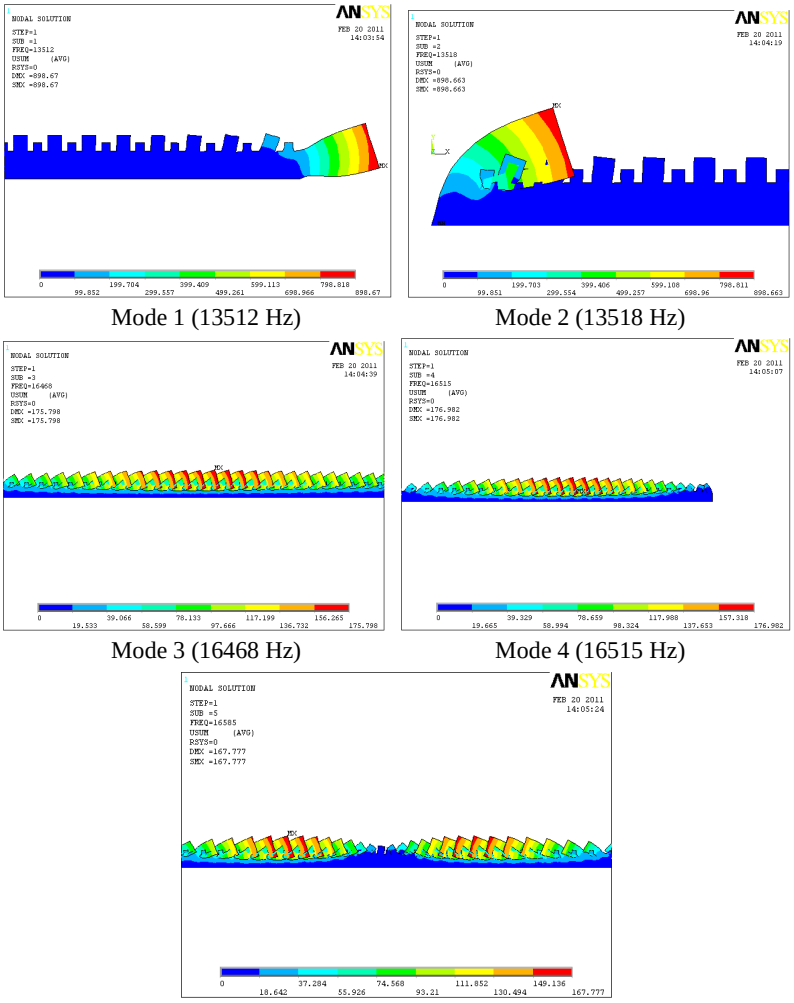

Mode 1 (13512 Hz) Mode 2 (13518 Hz)

Mode 3 (16468 Hz) Mode 4 (16515 Hz)

Mode 5 (16585 Hz)

Fig. 16. 2-D Mode shapes for the stator with inter poles

The results of the analysis provide the displacements on stator for a given frequency range due to the normal and tangential forces. The forces developed depend on the excitation current and its shape. In the LSRM, the current is non-sinusoidal in shape and it contains harmonic components. These harmonic components generate forces on the stator in their respective frequencies. Fig. 25 shows the measured current and voltage waveforms using the Fluke

harmonic analyzer. The harmonic content of the current waveform is shown in Fig. 26 for the stator with pole shoe structure.

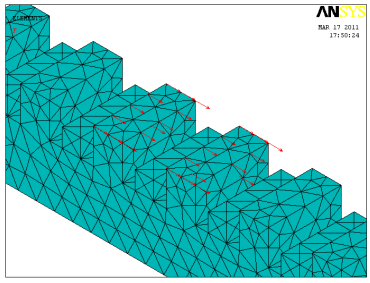

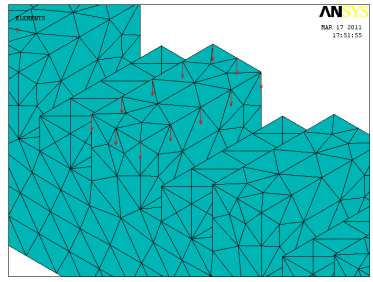

Fig. 17. Tangential force applied to the stator poles **Fig. 18.** Normal force applied to the stator poles

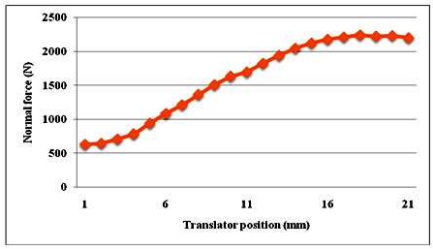

Fig. 19. Stator normal force profile

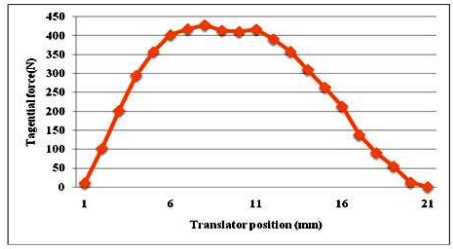

Fig. 20. Stator tangential force profile

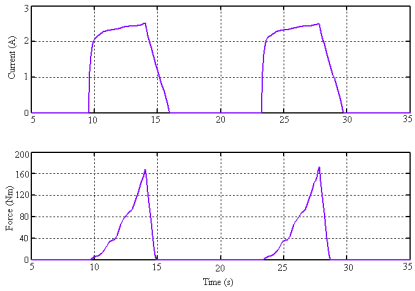

Fig. 21. Current and Normal force during the dynamic operation

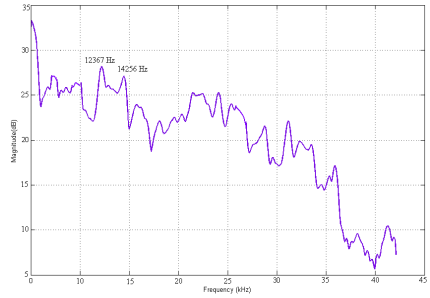

Fig. 22. Normal force spectrum

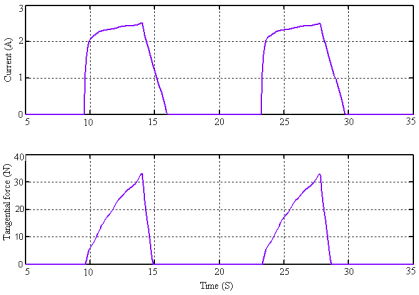

Fig. 23. Current and tangential force during dynamic operation

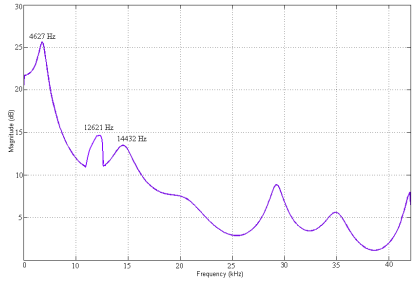

Fig. 24. Tangential dynamic operation force spectrum

The normal and tangential forces are calculated using the magnetic 2-D FEA for the current harmonic frequencies. The 3-D structural harmonic analysis is performed by using the calculated

forces and their frequencies as inputs. The result of the simulation is the vibration on the motor due to non-sinusoidal currents.

4. 6. 2. Vibration Due to Normal Force

The calculated normal forces are applied to stator inner surface and the structural harmonic analysis is performed to estimate the vibration frequency and magnitude. The fixing of stator on the base is defined in the analysis using displacement vector as zero. The boundary condition applied for the structural analysis is shown in Fig. 27.

The simulation result gives the displacement vectors acting on stator in the *X* and *Y* directions due to the normal force, shown in Fig. 28. It is estimated from the analysis that the vibration frequencies are high at 13750 Hz (near to first mode) in the *X* direction and in the *Y* direction. The maximum vibration amplitude in the *X* direction is 2.25µm at 13750 Hz (mode1 frequency) when the normal force is applied. The maximum vibration amplitude in the *Y* direction is 0.42 µm at 13750 Hz. From the simulation result it is observed that the vibration amplitude is high in the *X* direction, when the normal force is applied to the stator.

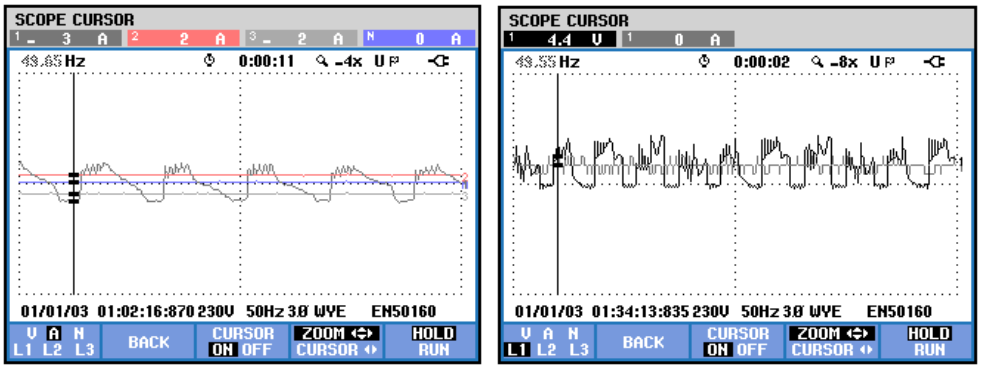

(a) Current waveform (b) Voltage waveform

Fig. 25. Measured current and voltage waveforms

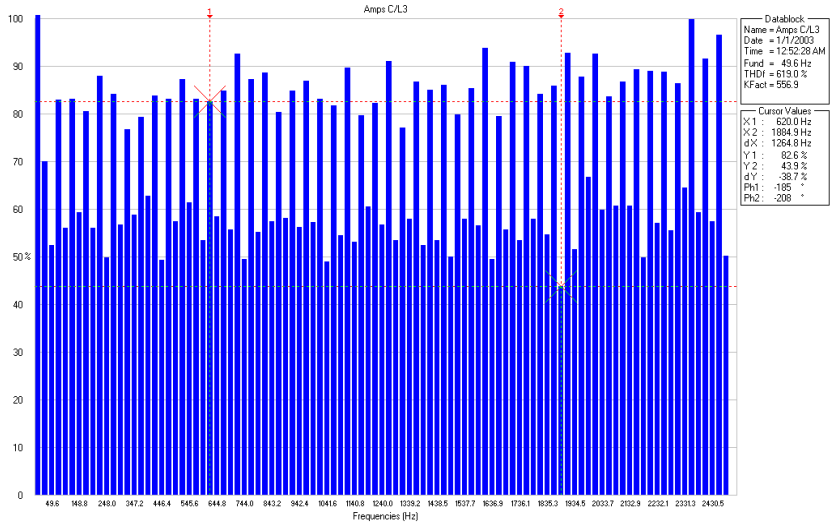

Fig. 26. Harmonic component of the current waveform

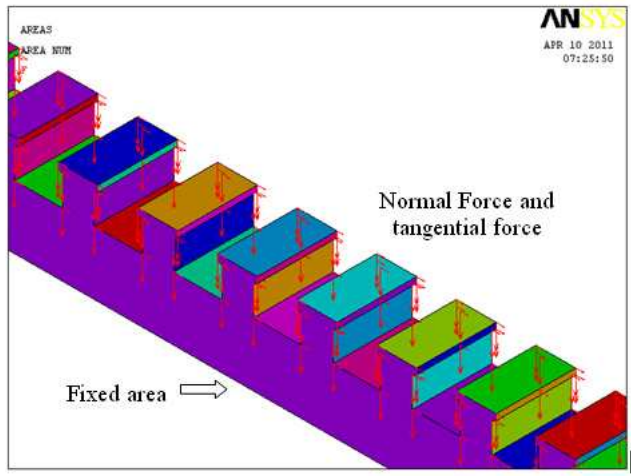

Fig. 27. Load applied on the stator for structural harmonic analysis

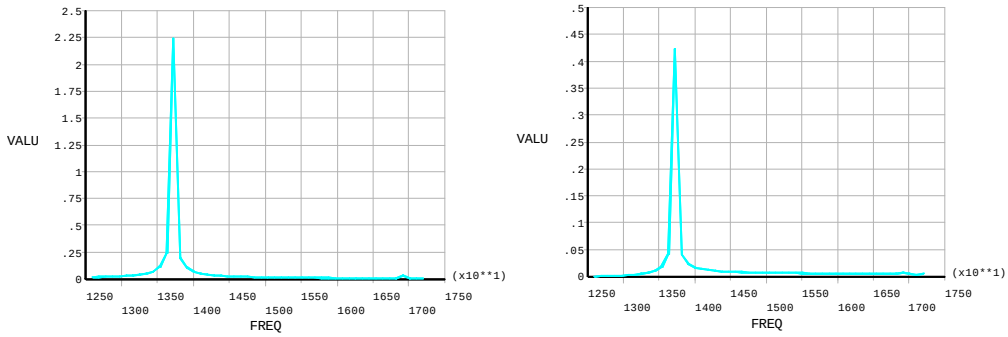

Fig. 28. Displacement on *X* and *Y* direction vs. frequency due to the normal force

4. 6. 3. Vibration Due to Tangential Force

To compute the vibration produced due to tangential force, at first the applied normal force is removed and the tangential force is applied on the stator. The displacements over the frequencies in *X* and *Y* directions are shown in Fig. 29. The maximum vibration amplitude in the *X* direction is 3 µm at 16900 Hz when the tangential force is applied. The maximum vibration amplitude in the *Y* direction is 0.97 µm at 16900 Hz.

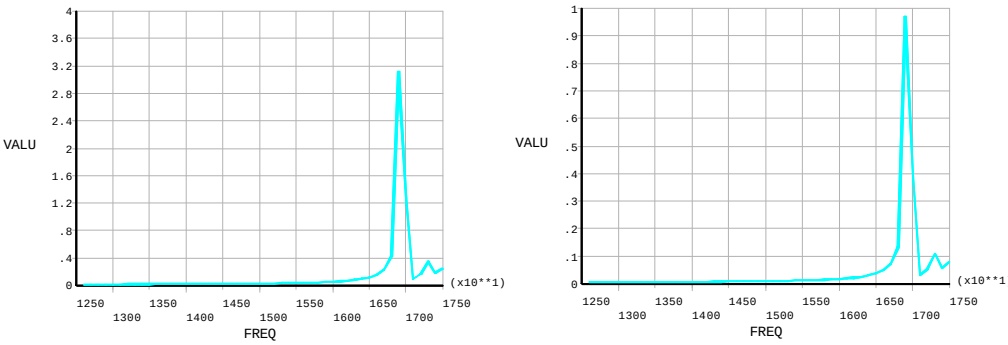

Fig. 29. Displacements on *X* and *Y* direction vs. frequency due to the tangential force

Finally, it is concluded that the amplitude of vibration is high in the *X* direction when the normal force is applied to the stator. To avoid resonance during the operation, the LSRM should not be operated at 13750 Hz (first mode frequency) and 16900 Hz (third mode frequency).

5. Experimental Results

The vibration generated in the motor is measured using the accelerometer to validate the estimations. Fig. 30 shows the block diagram of the experimental arrangement. To measure the vibration, the accelerometer is mounted on the surface of the stator. The measurement is taken using the Mixed Signal Oscilloscope (MSO). The operating frequency of the accelerometer is selected according to the switching frequency. Figs. 31-33 show the measured acceleration and its spectrum on the stator surface for the three structures.

It is observed from the experimental results that the spectrum contains a set of frequencies. The magnitude of the vibration is high at 12638 Hz (nearer to the first mode) and 14,676 Hz (nearer to the third mode) on the stator surface of the LSRM with pole shoes.

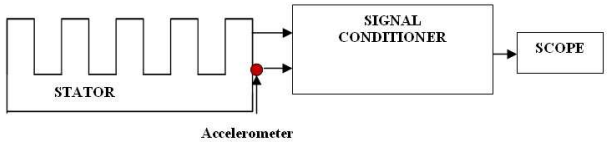

Fig. 30. Experimental arrangement

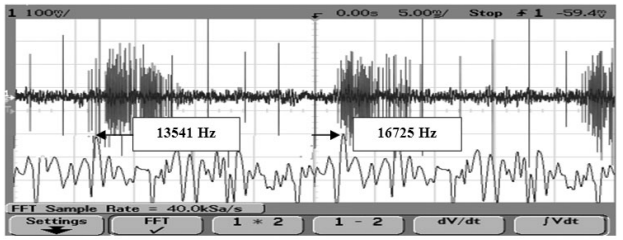

Fig. 31. Acceleration on the stator surface and its spectrum for the basic structure

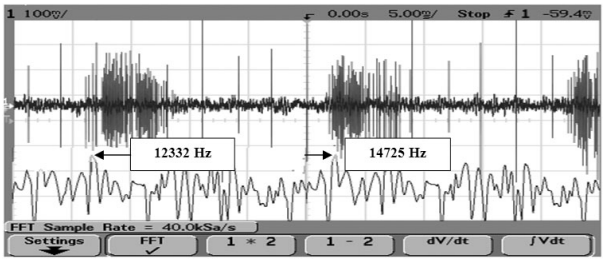

Fig. 32. Acceleration on the stator surface and its spectrum for the stator with inter poles

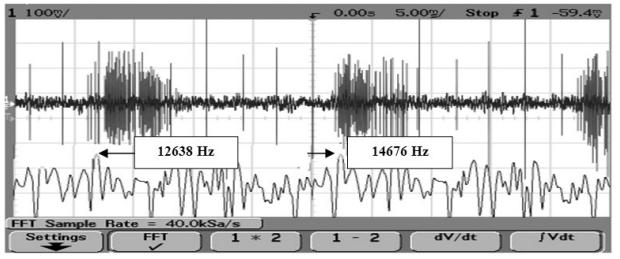

Fig. 33. Acceleration on the stator surface and its spectrum for the stator with pole shoes

6. Conclusion

An approximate formula has been derived to compute the natural frequency of the LSRM. The formula is shown to be accurate by comparison with the FEA, and hence is useful in preliminary design studies to evaluate the impact of vibration and acoustic noise. Analysis reveals that the LSRM stator with pole shoes has better vibration effect over other two structures. The vibration frequencies predicted due to the normal forces nearly matches with the vibrations produced on the stator side measurement. The differences may be due to the assumptions in the analysis and also partially due to the exclusion of other supporting components such as wheel housing in the simulation model.

References

[1] **Cameron D. E., Jeffrey Lang H., Stephen Umans D.** The origin and reduction of acoustic noise in doubly salient variable-reluctance motors. IEEE Transactions on Industry Applications, Vol. 28, No. 6, 1992, p. 1250-1255.

[2] **Chu F. H., Wang B. P.** Experimental determination of damping in materials and structures. Proc. ASME Winter Annual Meeting Chicago. Issue 38, 1980, p. 113-122.

[3] **Ewins D. J.** Modal Testing: Theory, Practice and Application (Mech. Engg. Research Studies; Engg. Dynamics Series). UK. Willey Publishers, 2001.

[4] **Girgis R. S., Verma S. P.** Method for accurate determination of resonant frequencies and vibration behavior of stators of electrical machines. IEEE Proc. on Electric Power Applications, Vol. 128, No. 1, 1981, p. 1.

[5] **Joon-Ho Lee, Young-Hwan Lee, Dong-Hun Kim, Ki-Sik Lee, Il-Han Park** Dynamic vibration analysis of switched reluctance motor using magnetic charge force density and mechanical analysis. IEEE Transactions on Applied Superconductivity, Vol. 12, No. 1, 2002, p. 1511-1514.

[6] **Srinivas K. N., Arumugam R.** Analysis and characterization of switched reluctance motors, Part II: Flow, thermal, and vibration analyses. IEEE Transactions on Magnetics, Vol. 41, No. 4, 2005, p. 1321-1332.

[7] **Verma S. P., Balan A.** Measurement techniques for vibration and acoustic noise of electrical machines. Proceedings of 6th International Conference on Electrical Machines and Drives, Oxford, UK, 1993, p. 546-551.

[8] **Verma S. P., Balan A.** Electromagnetic surface excitation system for the study of vibration behavior of stators of electrical machines. Proceedings of International Conference on Electrical Machines, Vigo, Spain, Vol. 1, p. 332-337.

[9] **Verma S. P., Girgis R. S.** Considerations in the choice of main dimensions of stators of electrical machines in relation to their vibration characteristics. IEEE Transactions on Power Apparatus and Systems, Vol. 94, No. 6, 1975, p. 2151-2159.

[10] **Yung Ting, Liang-Chiang Chen, Chun-Chung Li, Jeng-Lin Huang** Traveling-wave piezoelectric linear motor, Part i: The stator design. IEEE Transactions on Ultrasonic's, Ferroelectrics and Frequency Control. Vol. 54, No. 4, 2007, p. 847-853.